SIMULATION OF THE TDRS MULTIPATH ENVIRONMENT

DECEMBER 1970

Prepared Under
Contract NAS 5-10797
Multipath Signal Model Development

For
National Aeronautics and Space Administration
Goddard Space Flight Center
Greenbelt, Maryland 20771

Technical Memorandum G-161-10

SIMULATION OF THE TDRS MULTIPATH ENVIRONMENT

By

Dr. E. J. Baghdady
Dr. A. F. Ghais
R. H. Wachsman

December 1970

Prepared Under

Contract NAS5-10797

Multipath Signal Model Development

For

National Aeronautics and Space Administration
Goddard Space Flight Center
Greenbelt, Maryland 20771

ABSTRACT

This report discusses design principles and implementation methods for simulating the propagation path between a Tracking and Data Relay Satellite and a mission spacecraft. The emphasis is on multipath and doppler simulation but additive disturbances are also considered. The recommended form of the simulator is such that it is fed separately with the unmodulated carrier, the unmodulated subcarriers (or spread-spectrum components) and the data signals. The perturbations are also introduced separately; then successive modulation operations are performed.

The simulator is segmented into elements that perform the various functions of direct and specular multipath, diffuse fading, doppler shift and delay spread. Delay spreads are realized by discrete delays operating on baseband signals. Doppler simulation and ionospheric or diffuse multipath fading are applied to individual paths before or after modulation of the carrier by delayed baseband signals. Block diagrams are presented on how the different elements are combined to create a complete channel simulator.

TABLE OF CONTENTS

LIST OF ILLUSTRATIONS

LIST OF ILLUSTRATIONS (Continued)

Technical Memorandum G-161-10

SIMULATION OF THE TDRS MULTIPATH ENVIRONMENT

1. INTRODUCTION

As part of laboratory evaluation of any TDRS system, its susceptibility to multipath interference should be tested under realistictically simulated multipath propagation conditions. The desirable attributes of such a simulator are its relevance, its realism, and its flexibility.

The simulator's relevance is its ability to simulate only those channel properties that are central to the TDRS problem and to omit any properties that have no bearing on it. Thus its relevance could arise only from a deep understanding of the manner in which the channel can be expected to interact with the TDRS system. The simulator's realism is its ability to simulate a wide variety and range of expected channel conditions, within the bounds of economy and simplicity. Thus its realism would result from the generality and adequacy of the mathematical models underlying the simulator. Finally, the simulator's flexibility is its ability to support the full variety of experiments that might be contemplated for a TDRS system. Thus its flexibility depends on appreciation of the types of tests that should be performed on the TDRS system.

The purpose of this memorandum is to describe relevant, realistic and flexibile techniques for the simulation of the TDRS multipath environment.

The memorandum is organized as follows: We begin in Sec. 2 with a brief discussion of the technical background of the TDRS system, especially as it relates to channel simulator requirements. The general approach to the channel simulator problem is then outlined in Sec. 3, preparing the way for

more detailed discussions in ensuing sections. In Sec. 4 techniques for simulating the various channel properties are first outlined, then tentative selections amongst these techniques are made on the basis of feasibility of implementation with state-of-the-art components, as well as on relative complexity and flexibility. This then leads, in Sec. 5, to the description and discussion of a complete channel simulator configuration that embodies all the preceding considerations and tentative selections. A simulator, which is particularly suited to the wideband FM system for which the independently fading sideband diffuse multipath model is valid (see Sec. 5 of Technical Memorandum G-161-6) is presented in Sec. 6.

2. TECHNICAL BACKGROUND

The TDRS system is intended to become the primary communication link between low-orbit spacecrafts and ground-based command and data acquisition centers. The system functions encompass not only the relay of uplink (commands) and downlink (telemetry) data, but also of tracking signals. Range and Range Rate tracking requires the preservation of phase and frequency or doppler information through the TDRS as well as through the uplink and downlink channels. The latter functions may prove to be the more demanding in terms of system complexity and sophistication, as compared with the more familiar data-relay functions.

Another fundamental function of the TDRS system is to accommodate a large number of spacecrafts simultaneously. This involves multiple access into the TDRS by numerous mission spacecrafts, and also the ability of each mission spacecraft to communicate with more than one relay satellite. Signaling techniques enabling multiple access operation, addressing, and smooth handover between relay satellites are under consideration for eventual inclusion in the TDRS system. Such signaling techniques include pseudo-noise codes used to phase modulate or to control the frequency-hopping of the RF carrier, and wideband FM modulation.

A variety of sources of disturbances can be expected to interfere with the functioning of a TDRS system. The channel disturbances are primarily:

a) Multipath propagation between the TDRS and the mission spacecraft, in both directions.

b) Radio interference from earth-bound sources.

c) Interference from satellites in the multi-user and multi-TDRS environment other than the desired pair.

d) Ionospheric and tropospheric propagation effects on the desired signal.

It is clear that any TDRS system will employ sufficiently new communications techniques, and be subjected to sufficiently unfamiliar combinations of disturbances to warrant careful evaluation on the ground prior to finalization as space hardware. This evaluation consists first of systematic analysis of the expected performance of proposed system concepts under the most realistic models of the actual operating conditions; then, once a system concept or concepts have been selected, their critical portions must be experimentally evaluated under simulated channel conditions. This is the most immediate need for the channel simulator under discussion, although it serves numerous other needs as the TDRS program progresses past the system definition phase. Specifically, the simulator enables the judicious selection between competing system concepts prior to the development of space hardware, and does so far more definitively than any theoretical analysis could.

The above discussion helps to motivate the full variety of tests that could be performed on a TDRS system with the help of a channel simulator. The performance of the system in accomplishing its various functions could be tested under the full range and variety of expected channel conditions. Thus, data transmission, both command and telemetry, as well as round-trip tracking could be tested, in terms of suitable performance criteria. In addition, other tests not commonly performed could be conducted here; namely, tests of signal acquisition in the presence of disturbances, and tests of user handover from one TDRS to another.

The simulation should embody all the sources of disturbances listed in (a) through (d) above, as well as all the more customary operating conditions such as signal strengths, additive noise levels, doppler dynamics, etc. Simulation enables the "dynamic arrest" of channel conditions, so that appropriate observations of system performance can be made that would otherwise be impossible. In subsequent stages of testing, however, it is valuable to simulate continuously-varying conditions such as would be met in a typical satellite "pass."

The simulator described in this memorandum is limited to a one-way channel, but expandability to two-way channels is an important consideration in the selection of simulation techniques and their implementation. Similarly, the simulator operates with pre-set channel conditions or parameters, thus holding the channel in a state of dynamic arrest; but the programmability of these parameters by external automatic means is a highly desirable property.

3. GENERAL APPROACH

In this section we outline Teledyne ADCOM's general approach to the channel simulator problem, thus preparing the way for more detailed discussions in ensuing sections of the various elements of the approach. Here, we discuss the degree to which the various disturbances should be simulated, the general interfacing of the simulator with the outside world, as well as the manner in which the channel parameters should be set. Later sections will deal in detail with the channel models underlying the simulation, techniques for simulating the various channel attributes, and typical configurations of a complete channel simulator.

3.1 Disturbances to be Simulated

Of all the disturbances listed in Sec. 2 to which a TDRS system will be subjected, multipath propagation is the most demanding in terms of simulation techniques. We place great emphasis in this memorandum on multipath simulation, including ionospheric and tropospheric effects. Additive disturbances, including noise, earth-emanating interference, and interference from other spacecrafts utilizing the TDRS system are readily simulated using appropriate signal sources external to the channel simulator.

The various attributes of multipath propagation to be simulated are discussed in detail in Sec. 4. The degree to which each should be simulated is carefully considered in terms of its relevance, realism and flexibility. Suffice it to indicate here that the multipath simulation should include a direct path, specular reflection path, and diffuse multipath components.

Simulation of overall doppler shift deserves special mention here. Strictly speaking, doppler is an attribute of the link terminals, i.e., either

the user transponder or relay sateelite. In a simulation of the two-way channels, it is most realistic to incorporate the overall doppler in the transponder simulator. However, in the limited context of one-way channel simulation, overall doppler should be included in the channel simulator. This is because it will be desired in the system tests to introduce a calibrated doppler shift external to the satellite equipments, in order to test for doppler effects while at the same time utilizing the transmitted carrier as frequency reference.

3.2 Channel Simulator/TDRS System Interface

The desired channel simulator is a "throughput" simulator, that is, it accepts an RF or IF carrier modulated by one of a number of possible modulation formats, and delivers a perturbed version of this carrier at the output. The simulation approach that immediately suggests itself is to introduce the various disturbances directly onto the input carrier without resorting to any decomposition into unmodulated carrier, baseband and data signals. Unfortunately, this seemingly straightforward approach is fraught with difficulties which are explained in detail in Secs. 4 and 5. Here, we simply allude to these difficulties, and indicate the alternative approaches to circumventing them.

The difficulties involved in simulating multipath propagation in a TDRS system directly at the RF or IF are primarily in the simulation of a differential delay, delay spread, and to a lesser extent differential doppler and doppler spread. Introduction of these disturbances at RF with a wide, accurate and flexible variation of the respective parameters, is almost impossible within the limitations of state-of-the-art components. It is necessary to exploit the detailed structure of the signals to accomplish adequate simulation.

Whatever the type of final modulation on the carrier, whether it is AM, PM, FM, etc., the modulating signal itself is generally a composite of relatively narrowband data signals and relatively wideband subcarrier signals.

By subcarricer signals is meant here intermediate signals in the modulation chain between the data signals and the carrier. They need not be sinusoidal like the most common form of subcarrier. They could be pseudorandom sequences, or periodic clock sequences. They are used for multiplexing, for ranging or range-rate measurement, for spreading the spectrum, or for any combination of these purposes.

Now, there are three alternatives available for the introduction of the channel perturbations, according to the form in which the unperturbed signals are introduced to the perturbing operations; namely,

a) The straightforward approach of operating directly on the modulated carrier. The difficulty with this approach has already been mentioned.

b) The simulator is fed separately with the unmodulated carrier and the composite modulating signal. The perturbations are also introduced separately, then modulation operations are performed.

c) The simulator is fed separately with the unmodulated carrier, the unmodulated subcarriers (or spread-spectrum components) and the data signals. The perturbations are also introduced separately, then successive modulation operations are performed.

In the latter two alternatives, the convenient way to interface with the TDRS equipment is to feed the necessary signals directly from the transmitter exciter prior to modulation to the simulator, then back to the transmitter to form the direct-path signal. The specular and diffuse multipath signals require two (or possibly just one) auxiliary transmitters. These could either be incorporated in the simulator, or preferably be externally interconnected through a suitable interface with the simulator.

If the necessary signals are not readily available from the TDRS equipment, or if it is not desired to interface with the simulator through more than one input port and one output port, then the modulated carrier has to

be demodulated into its constituent. This, of course, is feasible to do, although somewhat cumbersome, since the various modulation techniques have to be accommodated by parallel demodulation equipments in the simulator.

The main difference between alternatives (a) and (b) is that it is extremely convenient to introduce the perturbations on the data signals and the subcarriers separately, as will be seen in Sec. 5. Alternative (c) permits this, at the price of additional functional operations in the simulator. This is more than offset, however, by the relative simplicity of the individual operations. Consequently, alternative (c) is adopted with the provision that the necessary signals are fed directly from the TDRS equipment. This is reflected in the typical simulator configuration presented in Sec. 5.

3.3 Setting Channel Conditions

The simulator could have manual controls to set the various channel conditions, such as levels, dopplers, delays, etc. Thus the channel could be held in a state of dynamic arrest corresponding to the set of parameters selected. We do consider the external programmability of these parameters by automatic means a highly desirable capability for later implementation. In this way continuously-varying conditions, such as would be met in a typical satellite pass, could be simulated. A computer-control interface could vary the parameter settings according to input data about the orbits of the user spacecraft and the TDRS. To do this it is necessary to ensure that the manual control elements can be converted to automatic drive. Digital drive is particularly convenient in this regard, wherever feasible.

4. SIMULATION METHODS OF CHANNEL DISTURBANCES

For analytical purposes, the signals received via the direct and reflected paths mentioned in the preceding sections can be expressed either as a specular response, as a diffuse response, or as a linear combination of specular and diffuse components. A propagation mechanism yields a specular output if, in response to an input represented by $e_{in}(t)$, it yields

$$e_{out}(t) = K\, e_{in}(t - \tau_s) \qquad (1)$$

where the amplitude factor, K, and the time delay, τ_s, are both either strictly constant or approximately constant over a time interval of interest. K and τ_s will generally fluctuate for a direct path with scintillation effects caused by the ionosphere (and, occasionally, the troposphere).

A propagation mechanism is said to yield a diffuse output if, in response to a single-frequency test signal it yields a large number of components that differ in amplitude, phase and/or frequency, but are of comparable strengths so that the properties of their resultant are not significantly influenced by the behavior of any single one of the components. When the differences among the components are random, the resultant will be nondeterministic. The statistical characteristics imparted to a signal by the random "diffusion" or "scatter" process of a propagation mechanism are generally non-stationary but they can be treated as approximately stationary over sufficiently short time intervals. With our description of a random-diffuse component, the central limit theorem of probability theory can be invoked to conclude that each sinusoidal component in the input of a pure scatter or diffusion process is transformed by such a process into an output that can be modeled as a sample function of a gaussian process.

The methods for simulating electronically the important propagation effects anticipated over a TDRS propagation channel will be described in the present section.

4.1 Simulation of Direct Path with Scintillation Effects

The various effects of transmission through the ionosphere (and occasionally through the troposphere) give rise to perturbations in amplitude by the time- and space-variant absorption properties and in phase by the corresponding time- and space-variant refractive fluctuations of the medium along the transmission path. In addition, there may arise some splitting of the direct path into several paths of nearly the same properties by atmospheric stratifications along the direct path.

The fluctuations in the densities of the constituents of the atmosphere (as functions of time and space variables) along a signal propagation path, give rise to fluctuating absorption and refraction effects. The absorption fluctuations are manifested in the amplitude of the signal, the variations of the refractive index cause ray bending, and hence path-length and angle of arrival changes from those of a straight line path connecting the transmitting and receiving points. The time-variant nature of even the more gradual changes in the absorption characteristics and the refractive index gives rise to a scintillation, or "twinkling," of the received signal amplitude and phase, respectively. The scintillation is significant for microwaves, particularly insofar as it contributes the path amplitude and phase variabilities that figure significantly in the interference among a multiplicity of simultaneous paths.

Of principal interest in the analysis of multipath effects and of phase and frequency sensitive signal operations is the effect of the variability of the refractive index in the portion of the atmosphere traversed by a single propagation path upon the phase stability of the signal. The basic relationship

between propagated signal phase along a single path and the refractive properties of the propagation medium stems from the fact that if $n(s, t)$ denotes the index of refraction along a path of length L, the transit time can be expressed as

$$\tau(t) = \frac{1}{c} \int_0^L n(s, t)\, ds$$

where s denotes distance along the path, the notation $n(s, t)$ expresses the dependence of the index of refraction upon both position along the path and time, and the variation of $n(s, t)$ with t is assumed to be sufficiently slow that during the transit time interval $n(s, t)$ does not change significantly. If we define

$$m_n(t) = \frac{1}{L} \int_0^L n(s, t)\, ds$$

then

$$\tau(t) = m_n(t)\, L/c$$

where $m_n(t)$ is recognized as the "spatial" mean value of $n(s, t)$ for the path of interest during the transit time interval centered about the time instant t. The transit-time phase shift of a sinusoidal carrier of wavelength λ can now be expressed as

$$\phi(t) = (L/\lambda)\, m_n(t) \qquad (2)$$

The received sinusoidal carrier will therefor portray random phase fluctuations, $\phi(t)$, with time if the atmosphereic conditions along the path cause the spatial-mean index of refraction $m_n(t)$ to fluctuate randomly in time. The intensity of the phase fluctuations naturally varies inversely with the wavelength of the propagated carrier for a given path defined by a nominal length L and a time-variant spatial-mean index of refraction, $m_n(t)$.

4.1.1 Simulation of One Direct LOS Path with Scintillation Effects

If the signal

$$e_{in}(t) = \cos \omega_o t \tag{3}$$

is radiated by the transmitting antenna, the signal received over a scintillating direct line-of-sight path can be expressed as

$$e_{dp}(t) = V(t) \cos[\omega_o t + \phi_o(t)] \tag{4}$$

where $V(t)$ represents the fluctuating envelope and $\phi_o(t)$ the phase fluctuations. Note that we can write

$$\phi_o(t) = \phi_{fast}(t) + \phi_{slow}(t) \tag{5}$$

where $\phi_{fast}(t)$ represents the relatively rapid "instant-to-instant" phase fluctuations, and $\phi_{slow}(t)$ represents the relatively slowly fluctuating average value (over a few seconds) of the phase. At VHF and S-band frequencies

$$\overline{\phi^2_{fast}(t)} \ll 1 \tag{6}$$

but $\phi_{slow}(t)$ may actually amount to relatively large drifts (up to a few times 2π or more depending upon the path length and the operating frequency) in a period of minutes. For two different operating frequencies f_1 and f_2 we would expect from Eq. (2) that if $\phi_k(t)$, $k = 1$ or 2, represents the total phase fluctuations in Eq. (4) then

$$\phi_2(t) = (f_2/f_1)\, \phi_1(t) \tag{7}$$

The probability distribution law that governs the instantaneous values of the phase fluctuations can be surmized as follows. We first associate the faster fluctuations represented by $\phi_{fast}(t)$ with the random fluctuations of

incremental contributions from successive spatial regions traversed by the signal over the propagation path. The slower drifts represented by $\phi_{slow}(t)$ are then associated with the relatively slow variations in the delay characteristics of larger spatial regions containing the path. If we further assume that the more rapidly variable incremental delays that make up $\phi_{fast}(t)$ are independent for the successive parts of the traversed path, and that they are all comparable in importance, then the central limit theorem suggests that the instantaneous values of $\phi_{fast}(t)$ obey a gaussian probability density function restricted practically to within an interval of width 2π. The total phase fluctuation $\phi_o(t)$ can therefore be treated as a gaussian process added to a slowly fluctuating median represented by $\phi_{slow}(t)$.

The probability distribution law governing the envelope fluctuations in V(t) can be surmised from the phenomenological cause of the fluctuations. Thus, if the phase fluctuations are correctly attributed to the time variations of the spatial-mean refractive index, $m_n(t)$, the envelope fluctuations must be attributed to the attendant time variations of the spatial-mean atmospheric absorption over the traversed path. The total attenuation sustained at a given instant of time may be considered as the result of a large number of independently variable elemental attenuations sustained in cascade along the traversed path. If the component increments of attenuation introduced over various parts of the propagation path are expressed in dB, the total attenuation in dB will be the sum of a large number of independent random components, the properties of each of which becomes lost in the properties of the total. From the central limit theorem, this concept of the composition of the total attenuation along the path suggests that the statistics of the envelope fluctuations should be log-normal; i.e., the fluctuations expressed in dB should be characterized by a gaussian probability distribution function. Specifically, if

V_t represents the value of V(t) at a particular instant of time, t, and if

$$\alpha_t = \ln V_t$$

then α_t is a random variable with a gaussian probability density function

$$p_\alpha(A) = \frac{1}{\sigma_\alpha \sqrt{2\pi}} e^{-(A-m_\alpha)^2/2\sigma_\alpha^2} \quad -\infty < A < \infty$$

where m_α is the mean value of $\ln V$, and σ_α is its variance. Accordingly, it is readily shown that

$$p_V(v) = \frac{1}{v\,\sigma_\alpha \sqrt{2\pi}} e^{-(\ln v - m_\alpha)^2/2\sigma_\alpha^2}, \quad v \geq 0$$

$$= 0, \text{ otherwise}$$

The preceding observations about the characteristics of the envelope and phase fluctuations for a single direct line-of-sight propagation path suggest the functional diagram shown in Fig. 1 for generating these effects in the laboratory.

4.1.2 Simulation of Ionospheric Multipath Effects on the LOS Signal

Path splitting in the ionosphere (or through the troposphere, at low elevation angles relative to the earth's surface) gives rise to a number of direct LOS paths in parallel, each having the characteristics described in Sec. 4.1.1 with small delay differences and relative amplitudes that may range between 0 and 1. In the case of an unmodulated carrier the relative delays among the various paths can be accounted for by slowly fluctuating carrier phase differences. Such multipath can therefore be simulated as illustrated in Fig. 2. Independent gaussian processes with properly shaped spectral density functions for the various paths can be derived from a single noise generator as illustrated in Fig. 3.

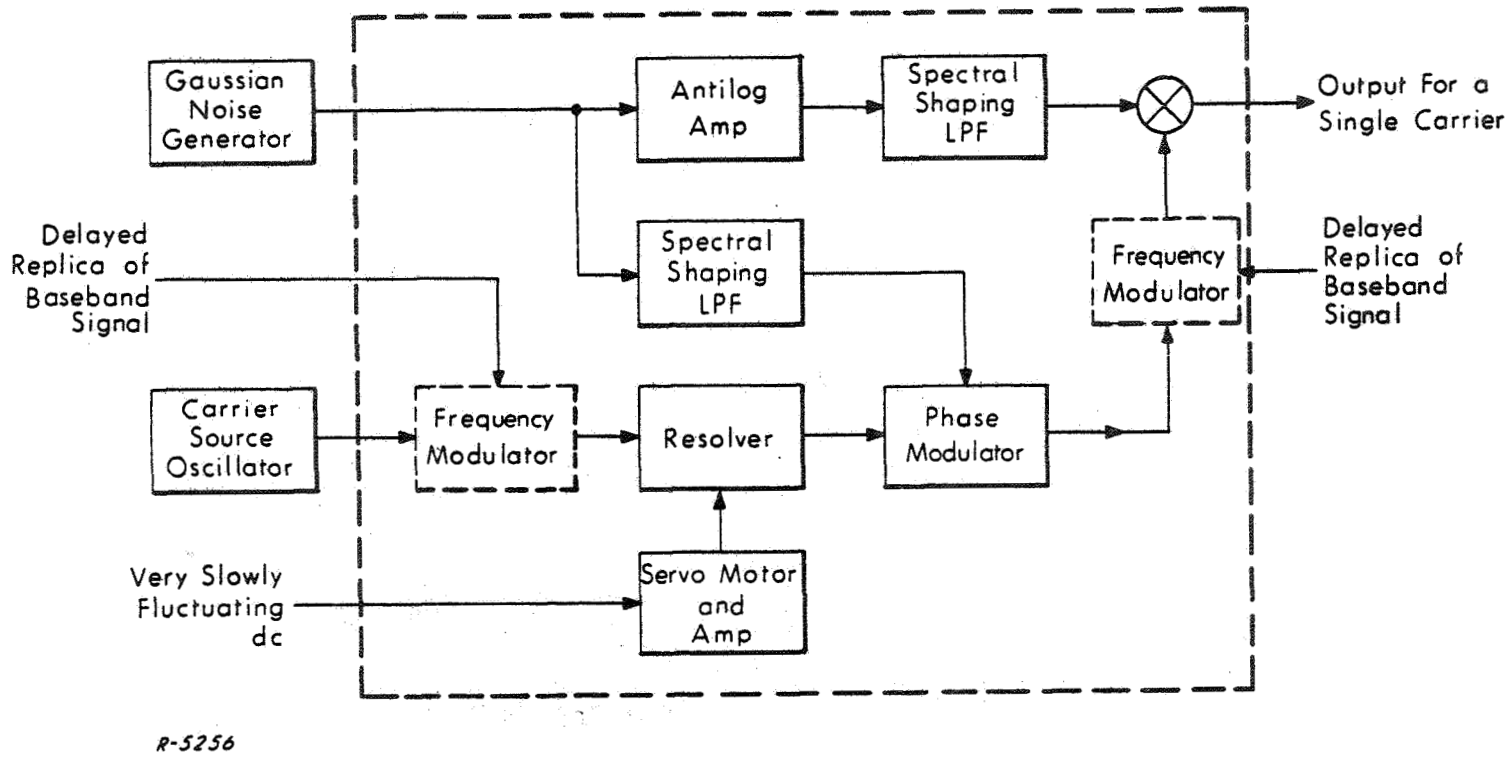

Fig. 1 Block Diagram for Generating the Propagation Effects Observed on a Single, Line-of-Sight Propagation Path. Alternate Locations of Modulation for a Frequency Modulation Application are Indicated by the Dashed Blocks.

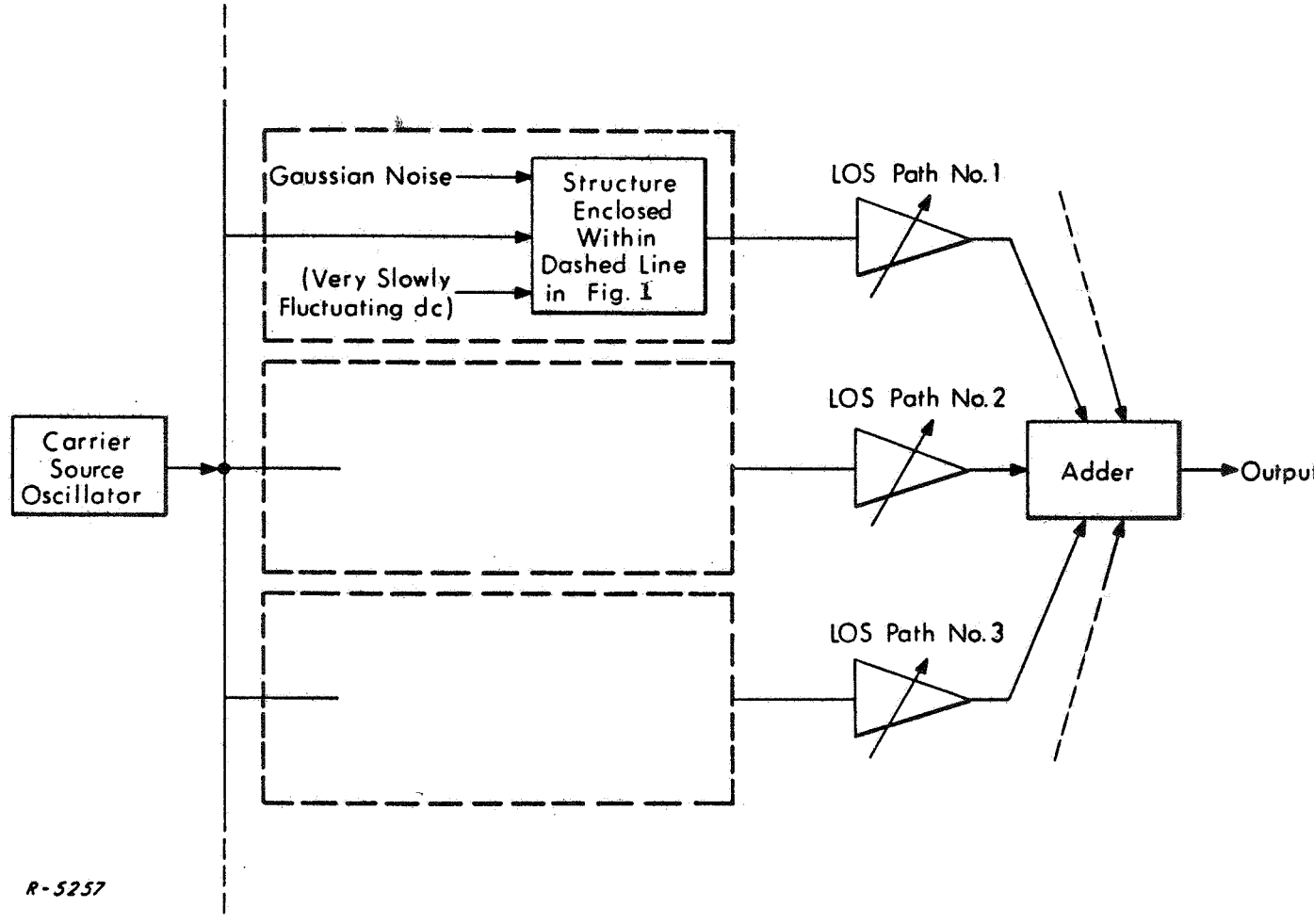

Fig. 2 Generation of LOS Atmospheric Multipath Propagation of an Unmodulated Carrier

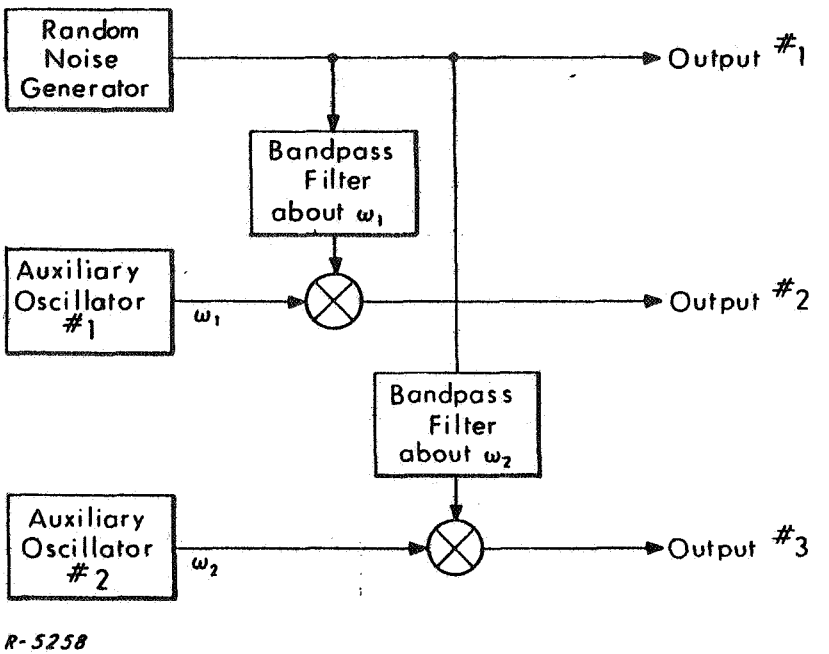

Fig. 3 Generation of Independent, Lowpass, Gaussian Noise Processes

In the case of a modulated carrier, the group delay differences among the various paths may have to be accounted for explicitly in the modulating signals.* Thus, if the modulating process is represented by g(t), then replicas of g(t) with relative time delays corresponding to the various paths are first obtained by means of a baseband delay line with appropriate taps. Each of these replicas is then used to modulate one of the atmospheric paths generated in Fig. 2. The resulting channel simulator appears as shown in Fig. 4. The blocks marked "modulator" perform the type of modulation of the propaged carrier that is desired in the simulation process. But while the arrangement in Fig. 4 may be satisfactory for linear modulation (AM, DSB, SSB, VSB, etc.), practical considerations for exponent modulation (FM, ϕM) require that the operation of modulation by the output of one of the baseband delay line taps be moved for each path either to between the blocks marked "Carrier Source Oscillator" and "Resolver" in Fig. 1, or to after the block marked "Phase Modulator" and before the introduction of the envelope fluctuations associated with the atmospheric medium in Fig. 1.

4.2 Simulation of Reflected Paths

Two types of reflections can be distinguished: specular, and diffuse. A specular reflection can be readily simulated as equivalent essentially to a direct scintillating path generated as illustrated in Fig. 1, with a group delay added to the modulating signal process and a random phase shift added to the carrier, relative to one of the regular direct atmospheric paths as a reference.

---

*This is only necessary if the modulation bandwidth is on the order of the direct-path coherence bandwidth.

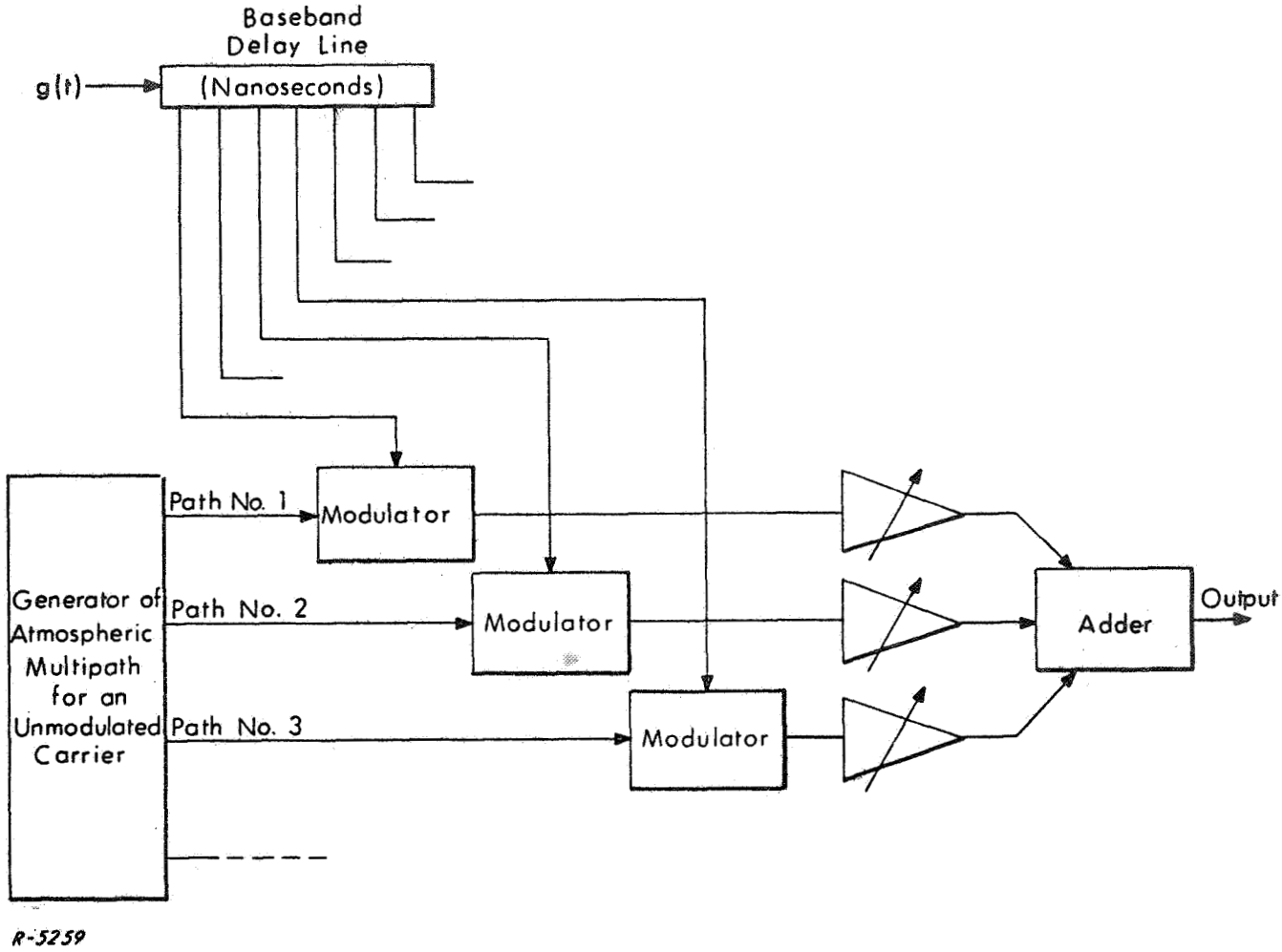

Fig. 4 Generation of LOS Atmospheric Multipath for a Modulated Signal

The method of generating a scatter-type or diffuse path response depends on the doppler-spread and delay-spread functions characteristic of the diffuse path to be simulated. The different types of diffuse paths defined by the doppler-spread and delay-spread functions may be identified as

a) path with nonzero doppler-spread shaped by a function that is symmetrical about the mean doppler shift, but with no significant delay spread;

b) path with nonzero doppler and delay spreads shaped by functions that are both symmetrical about their means;

c) path with no significant doppler spread but with a nonzero delay spread shaped by a symmetrical function; and

d) paths with nonsymmetrical spread function in either doppler or delay or in both.

The delay spread due to the spatial spread of the scattering earth's surface can be expected to be in the order of from several microseconds up to several milliseconds. Under these conditions, a diffusely reflected path can be simulated by the sum of several (five or more) suitably weighted paths as synthesized in Fig. 2 or 4. Delay differences between direct and reflected paths can be expected to be in the range between several microseconds and 30 milliseconds. Accordingly, a combination of a few atmospheric paths and one reflected path that is delay spread over tens of microseconds can be synthesized as illustrated in Fig. 5. The shape of the delay spread is determined by the settings of the variable-gain amplifiers shown. The doppler spread associated with reflections from a rough earth's surface can be accounted for by variations (among the components of the reflected path) in the rapidity of the "fluctuating dc" inputs to the "Servo Motor and Amp" blocks of the various component reflected paths indicated in Fig. 1.

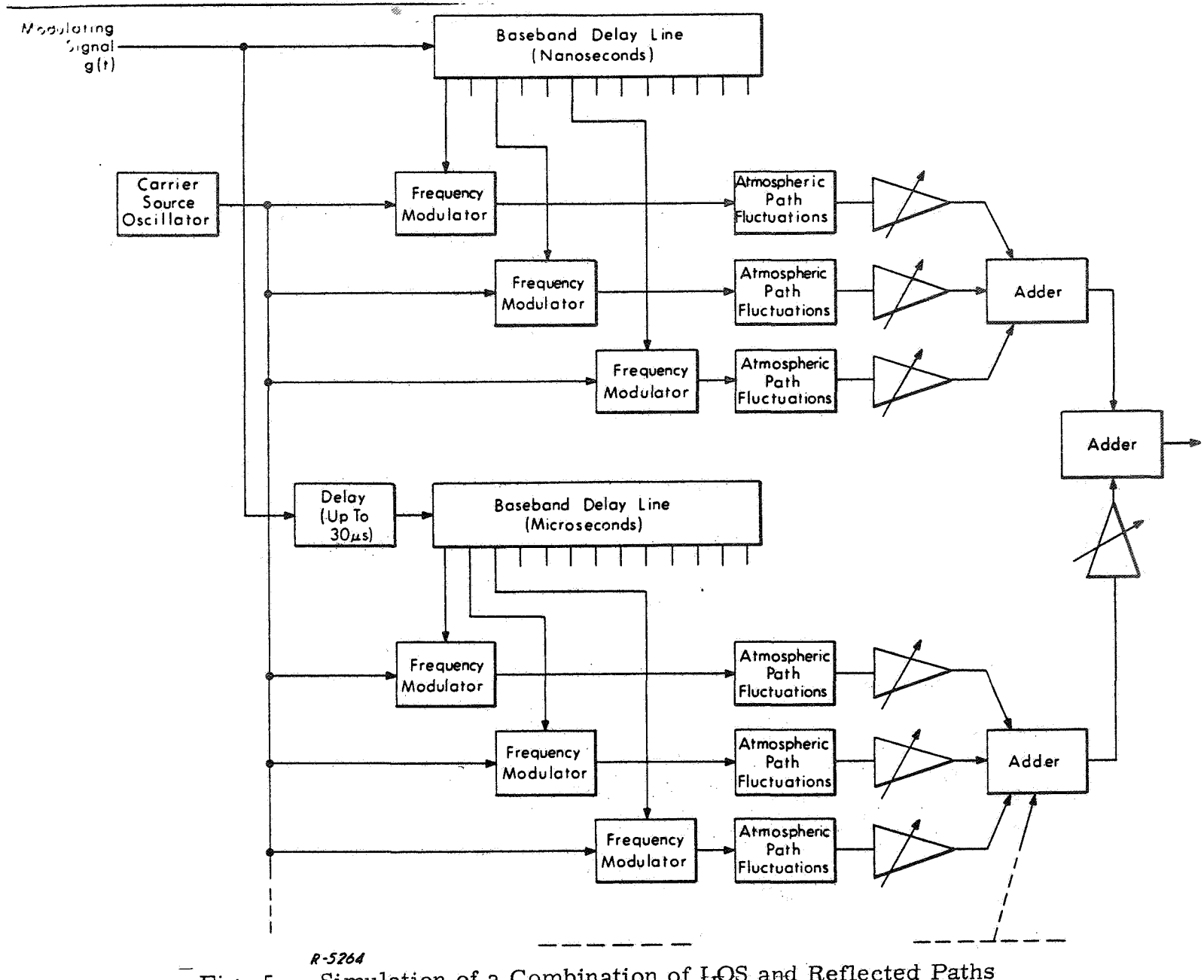

Fig. 5 Simulation of a Combination of LOS and Reflected Paths

The simulation of doppler spread characteristics with a specified shape and width of spectral density function over a continuous range of frequencies can be realized as shown in the following subsections for various types of modulation.

4.2.1 Symmetrical Doppler Spread and No Delay Spread

A straightforward technique for simulating a diffuse path characterized by a symmetrical doppler-spread function and no delay spread is presented in what follows. In Fig. 6(a), a technique is shown for generating the lowpass processes, $\{a_{nc}(t)\}$ and $\{a_{nq}(t)\}$, required for synthesizing the "cophasal" and "quadrature" components of a diffuse path. These processes are then used as shown in Fig. 6(b) to accomplish sinewave-to-gaussian conversion.

In Fig. 6, a gaussian noise generator yields an output with a white spectral density (or an approximation thereto). Independent narrowband gaussian fluctuations (usable in synthesizing different scatter paths as well as independent diversity channels) are extracted from the noise generator output by direct filtering of spectral zones centered at harmonics of some frequency ω_1. The output of the n^{th} bandpass noise filter can be expressed as

$$x_n(t) = x_{nc}(t) \cos n\omega_1 t - x_{nq}(t) \sin n\omega_1 t$$

Multiplication of the filter outputs by orthogonal pairs of sinewaves at the fundamental ω_1 and harmonics, $n\omega_1$, $n = 2, 3, \ldots$, of an "auxiliary relaxation oscillation" will yield the cophasal and quadrature components, $x_{nc}(t)$ and $x_{nq}(t)$ of each selected noise band down at zero Hz center frequency where each can be subjected to very narrow lowpass filtering to produce the desired shape and calibrated, selectable width of the fading spectral density of a

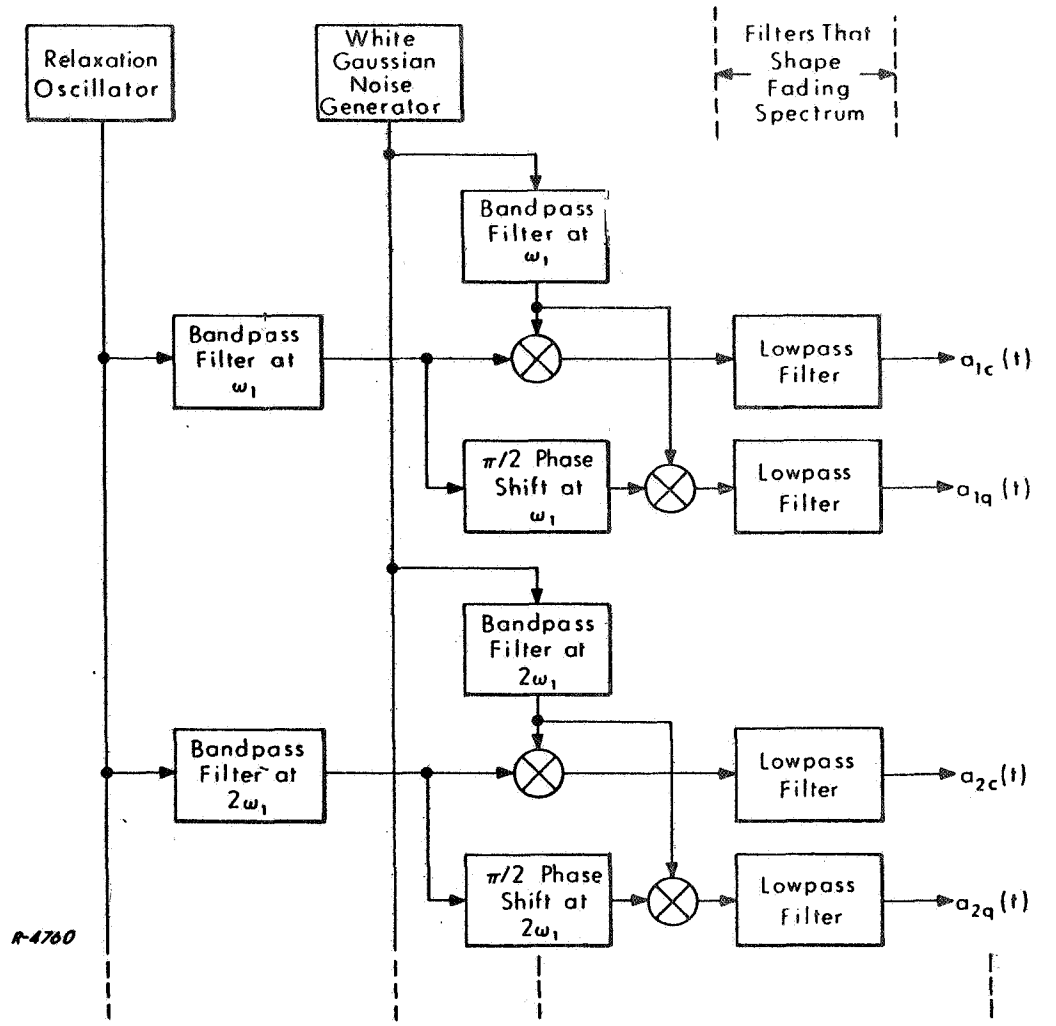

Fig. 6(a) Technique for Generating Cophasal and Quadrature Components of Spectrally Shaped Gaussian Noise for Different Diffuse Paths

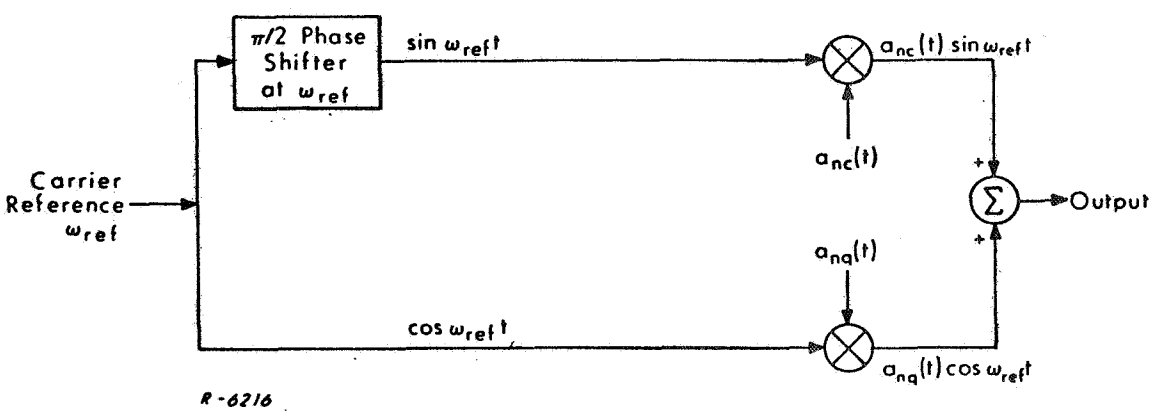

Fig. 6(b) A Method for Transforming a Sinusoidal Carrier or Signal Component into one with Gaussian Distributed Scatter-Type Fluctuations with a Symmetrical Doppler Spread Function and No Delay Spread

particular scatter path. The outputs of the lowpass filters in the various branches in Fig. 6 are slowly fluctuating waveforms,

$$a_{nc}(t) = x_{nc}(t) \otimes h_{\ell pn}(t), \qquad 2, 3, \ldots, N$$

and

$$a_{nq}(t) = x_{nq}(t) \otimes h_{\ell pn}(t), \qquad 2, 3, \ldots, N$$

having independent gaussian noise characteristics. The use of one or more additional "auxiliary relaxation oscillators" having fundamental frequencies different from ω_1 will allow many more of these slowly fluctuating gaussian-noise waveforms to be generated from the output of the same noise source. If the fundamental frequencies of the auxiliary relaxation oscillators differ by considerably more than the desired fading spectral widths, the resulting $a_n(t)$ fluctuations will be statistically independent. Selectable partial degrees of correlation between the random fluctuations of the various $a_n(t)$ waveforms can be obtained by bringing the relaxation oscillator frequencies closer together than the fluctuation bandwidths of the $a_n(t)$ waveforms.

4.2.2 Diffusion of AM and DSB Linear-Modulation Signals

The $a_n(t)$ waveforms of Fig. 6 can be used as illustrated in Fig. 7 to transform each sinusoidal component of an input AM or other DSB, linear-modulation signal into a "doppler-spread" scatter-type component with gaussian distributed instantaneous fluctuations.

In Fig. 7, the waveform, g(t), represents the desired lowpass base-band message function if the total signal to be transformed into a diffuse-path response is a linear-modulation, double-sideband signal expressible as $g(t) \cos \omega_{ref} t$. The outcome of the operations in Fig. 7 is

$$e_{DSB,\,diff}(t) = g(t - \tau_{dn}) \left[a_{nc}(t) \cos \omega_{ref} t - a_{nq}(t) \sin \omega_{ref} t \right]$$

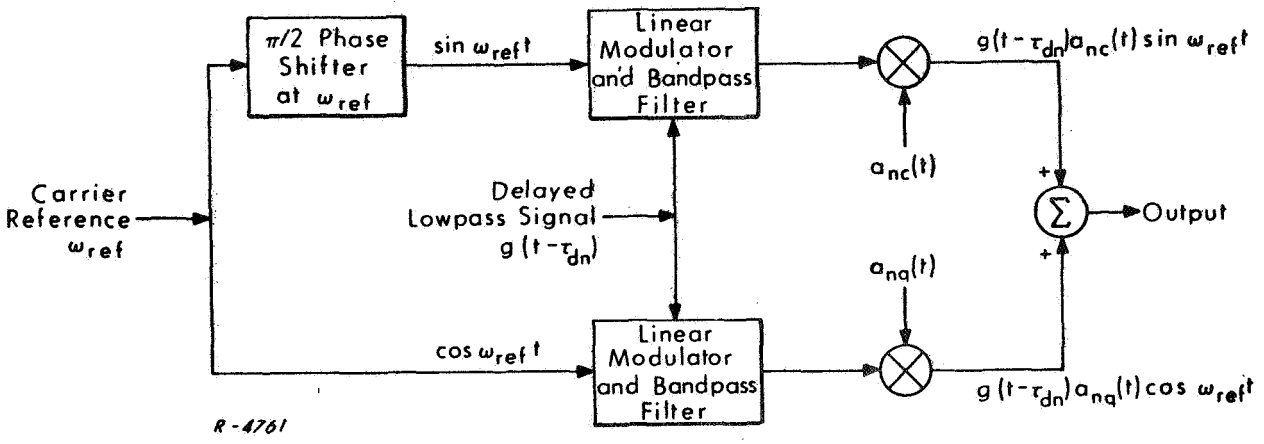

Fig. 7 A Method for Transforming a DSB Linear Modulation (AM and related DSB) Signal into one with Gaussian Distributed Scatter-Type Fluctuations with a Symmetrical Doppler Spread Function and no Delay Spread.

4.2.3 Diffusion of Exponent-Modulation Signals (FM or ϕM)

An exponent modulation signal is expressible as

$$e_{exp}(t) = \cos[\omega_c t + \psi(t)]$$

$$= \cos \psi(t) \cos \omega_c t - \sin \psi(t) \sin \omega_c t$$

The second line is recognized as the sum of two DSB signals with orthogonal reference carriers. Therefore, we conclude (by direct analogy with the DSB and SSB signals) that the outcome of diffusion with zero delay spread should be

$$e_{exp,\,diff}(t) = \cos \psi(t) [a_{nc}(t) \cos \omega_c t - a_{nq}(t) \sin \omega_c t]$$

$$- \sin \psi(t) [a_{nc}(t) \sin \omega_c t + a_{nq}(t) \cos \omega_c t]$$

$$= [a_{nc}(t) \cos \psi(t) - a_{nq}(t) \sin \psi(t)] \cos \omega_c t$$

$$- [a_{nc}(t) \sin \psi(t) - a_{nq}(t) \cos \psi(t)] \sin \omega_c t$$

These expressions suggest the operations shown in Fig. 8.

Alternately, we observe that since the delay spread is assumed to be zero, the coherence bandwidth is unlimited and we can readily write

$$e_{exp,\,diff}(t) = V(t) \cos [\omega_c t + \psi(t) + \phi(t)]$$

where $V(t)$ and $\phi(t)$ are the envelope and phase fluctuations introduced by the transformation of each sinusoidal component of the signal into a gaussian distributed component. For a doppler-spread function that is symmetrical about its mean, $V(t)$ is a sample function of a Rayleigh-distributed process

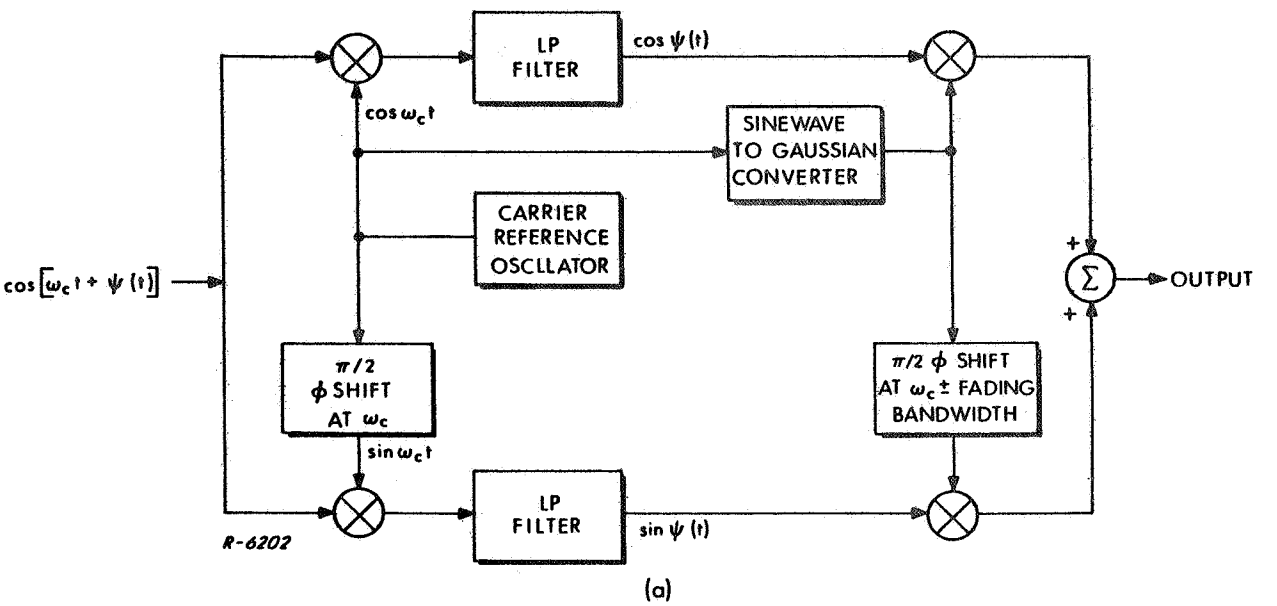

Fig. 8 Methods for Transforming a FM or ϕM Signal into one with Gaussian Distributed Scatter-Type Fluctuations with a Specified Doppler Spread (or fading spectrum) and no Delay Spread

and $\phi(t)$ is uniformly distributed over $|\phi| \leq \pi$, mod 2π. The above expression can be reqritten as

$$e_{exp,\,diff}(t) = a_{nc}(t) \cos [\omega_c t + \psi(t)] - a_{nq}(t) \sin [\omega_c t + \psi(t)]$$

where

$$a_{nc}(t) = V(t) \cos \phi(t) \text{ and } e_{nq}(t) = V(t) \sin \phi(t)$$

This last expression for $e_{exp,\,diff}(t)$ suggests the diffusion technique shown in Fig. 9.

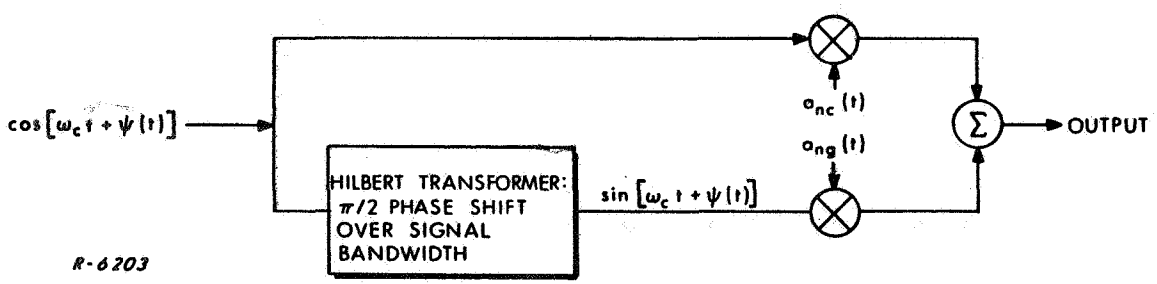

(b).

Fig. 9 Diffusion Technique

4.3 Overall Simulator Configuration

Two general approaches to the overall TDRS propagation simulator may be considered.

In the first, the various important channel parameters (such as differences in average delay and average doppler between the direct and the reflected paths, the nominal widths of the delay spread and the doppler spread of the reflected path) and the signal modulation parameters (such as modulation rate, modulated signal bandwidth) are scaled down, keeping constant fixed ratios among them. The result is a scaled-down model of the signal and the propagation parameters which generally makes it unnecessary to push the state-of-the-art of component developments (such as delay lines, modulators, etc.) in the implementation of an electronic simulator of the complete link. Special-purpose digital computer simulations can then also be made quite feasible and economically attractive within readily realizable computation speeds, switching times, sampling rates, etc. The principal shortcoming of this approach is that experimentation with actual terminal equipment connected through the propagation medium simulator may not be feasible because of the need for scaling down the modulation characteristics of the transmitting equipment and the design characteristics of the receiving equipment. Otherwise, the scaled-down-model simulator can provide a sufficient tool for the purpose of all investigations other than those requiring direct hook-up of actual "full-scale" equipment.

The second approach is the "full-scale" model simulator. Here, the channel parameters are assigned ranges of values that are expected in the actual medium.

In the discussions that follow, the configurations considered apply to either of the above approaches. But unless otherwise stated, the discussion will be directed to the "full-scale" model simulator.

4.3.1 General Functional Designs of TDRS Channel Simulator

A generic functional block diagram of the TDRS propagation channel simulator is shown in Fig. 10, where both the multipath propagation and the additive noise and interference are accounted for.

Inasmuch as the Statement of Work states that "the simulator should accept an RF or IF carrier ...," more detailed functional diagrams that capitalize on the practical advantages of introducing the delay differences and delay spreads at low frequencies must include RF or IF to low frequency interfaces and low-frequency to RF or IF interfaces. This is brought out in the functional diagram of Fig. 11.

In both Figs 10 and 11, the direct path is taken as reference with zero values of average delay and average doppler over time intervals on the order of a few seconds, only the delay and doppler differences between the direct and the reflected paths being of importance in effect on the tracking and data transmission performance during such time intervals. Absolute average doppler and delay values can of course be included, if desired, as when the effects of the dynamics of the relative motions of the synchronous and user satellites are of interest on the signal acquisition and tracking capabilities of the link equipment. The absolute "instantaneous" values of direct-path delay and doppler frequency shift can be introduced after the effects of interference between the direct and reflected paths have been accounted for, as illustrated by the dashed box in Fig. 11.*

4.3.2 Introduction of Delay-Shift and Delay Spread

The path group delays and delay spreads may conceivably be introduced into the RF modulated signal by means of one delay line for each path.

*Provision for nonzero average doppler is also considered in Sec. 5.

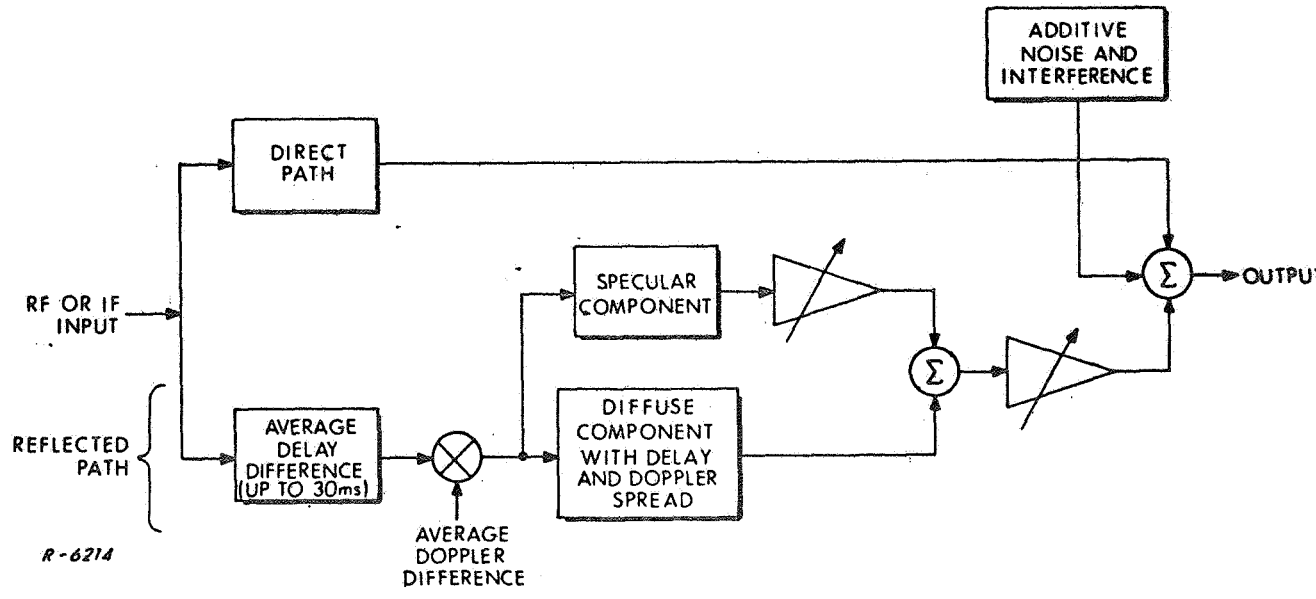

Fig. 10 Generic Functional Diagram of Overall TDRS Channel Simulator

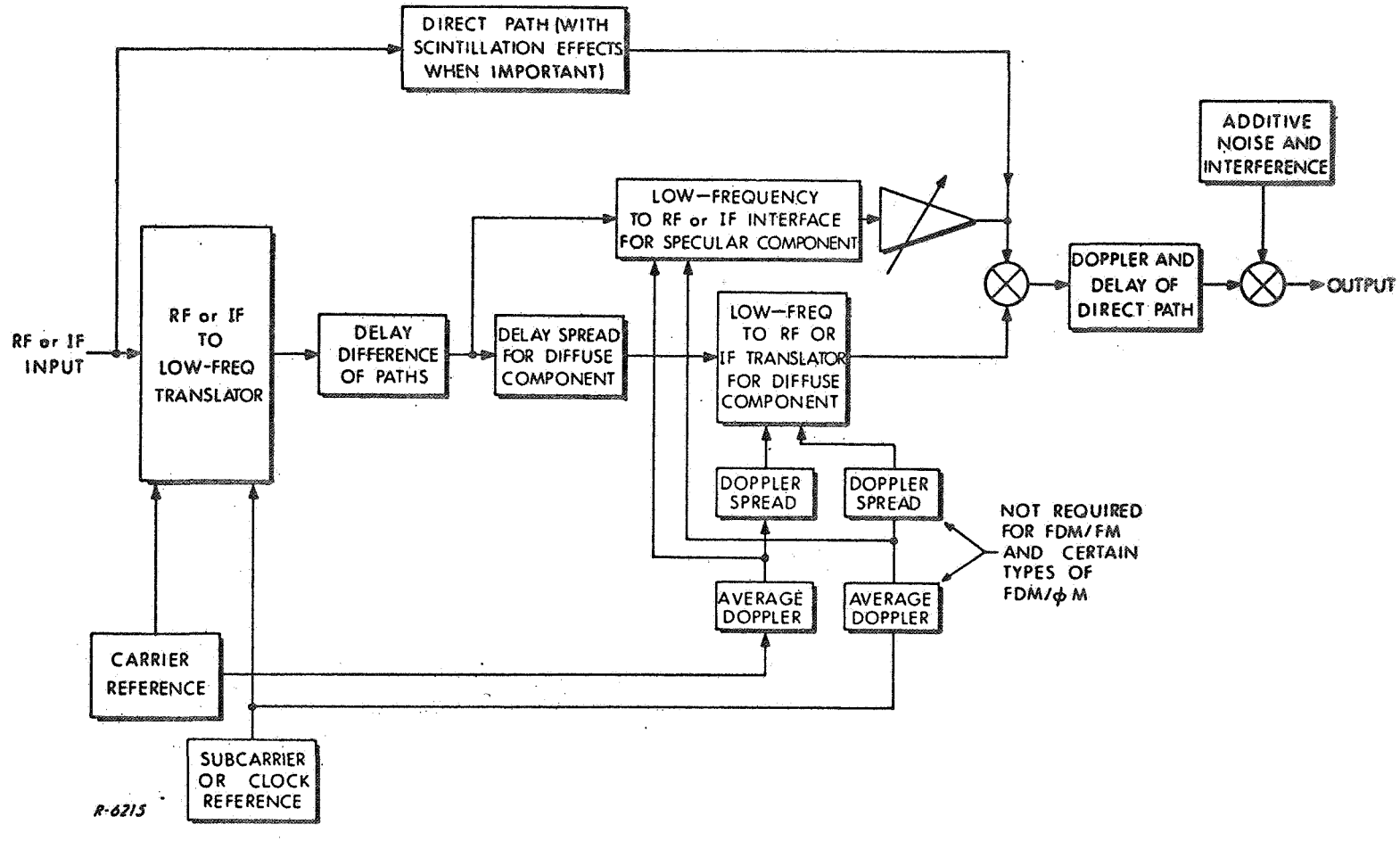

Fig. 11 Generic Functional Diagram Showing More Detailed Breakdown for RF and Low-Frequency Interfaces

This method of introducing delays is practically undesirable because the realization of large delays (up to 30 msec) in the laboratory at RF frequencies is combersome if not impracticable. Although this difficulty may be reduced by choosing a suitably low simulator operating frequency, the delay lines remain expensive at operating frequencies in the few megahertz, and other aspects of the realization of a satisfactory channel synthesizer are handicapped at such operating frequencies.

Thus, if the RF spectrum is translated first to a zero-hertz reference, (for AM and DSB) or the cophasal and quadrature components are translated down to zero-hertz reference (for FM and ϕM), a tapped low-frequency delay line can be used to provide baseband or low-frequency delay spreads of the type experienced over actual TDRS paths. Carrier delays are equivalent to random phase shifts which are absorbed in the random phase fluctuations of scatter components, and hence require special accounting only for specular components. Random settings of resolvers in the low-doppler generator of the simulator system and oscillator random walks in the high-doppler generator account for the required carrier random phasing from path to path. Carrier doppler shifts are introduced as calibrated frequency shifts of the signal from the main reference carrier oscillator. Each of the delayed baseband or RF to low-frequency translated signals product-modulates a doppler-shifted carrier signal to yield a translation of the low-frequency signal to the desired operating frequency range. The resulting modulated signal carries the desired delay of the baseband signal, the carrier doppler shift and the random carrier phase required for differences between different paths. The output signals from the reflected path synthesizer are added with the direct path, or reference path signal, and with the outputs of gaussian and interfering signal generators. The result is signal components and noises which can closely simulate those actually expected over TDRS links.

The introduction of delays and delay spreads at baseband or on low-frequency translates of the RF signal cophasal and quadrature components is highly suited for carrier modulations by

a) pseudo-random-noise (PN) codes (such codes can be delayed by arbitrary amounts simply by programming the "initial" settings of the maximal length code generator binary storage elements),

b) all combinations of PN codes and relatively narrowband information subsignals, and

c) all types of FDM systems combining narrowband data subchannels (for example, ADCOM's wideband FM spread-spectrum technique).

4.3.3 Doppler-Shift Simulation

Two different techniques may be used to simulate the low doppler (LD, i.e., 0 to 10 Hz) frequency shifts, and the high doppler (HD, i.e., 10 Hz and up) frequency shifts. A block diagram of a doppler-shift simulator is shown in Fig. 12. The low doppler shift (0 to 10 Hz) is obtained by using a motor-driven precision resolver which continuously shifts the phase of the synthesizer carrier reference signal at a rate proportional to the speed of the motor. Such resolvers operating at a 30 MHz carrier frequency are readily available commercially. Since these resolvers cannot simulate doppler over 10 Hz because of the limitation on permissible rotation speed, an alternate technique must be used to simulate doppler shifts above 10 Hz. One such technique is to add doppler plus a bias frequency, and then subtract the bias frequency. The bias frequency must be sufficiently large to enable effective separation of the sum and difference frequencies around the IF at the output of the mixers. The bias frequency must also be small enough so that the doppler frequency is much larger than the bias frequency instability.

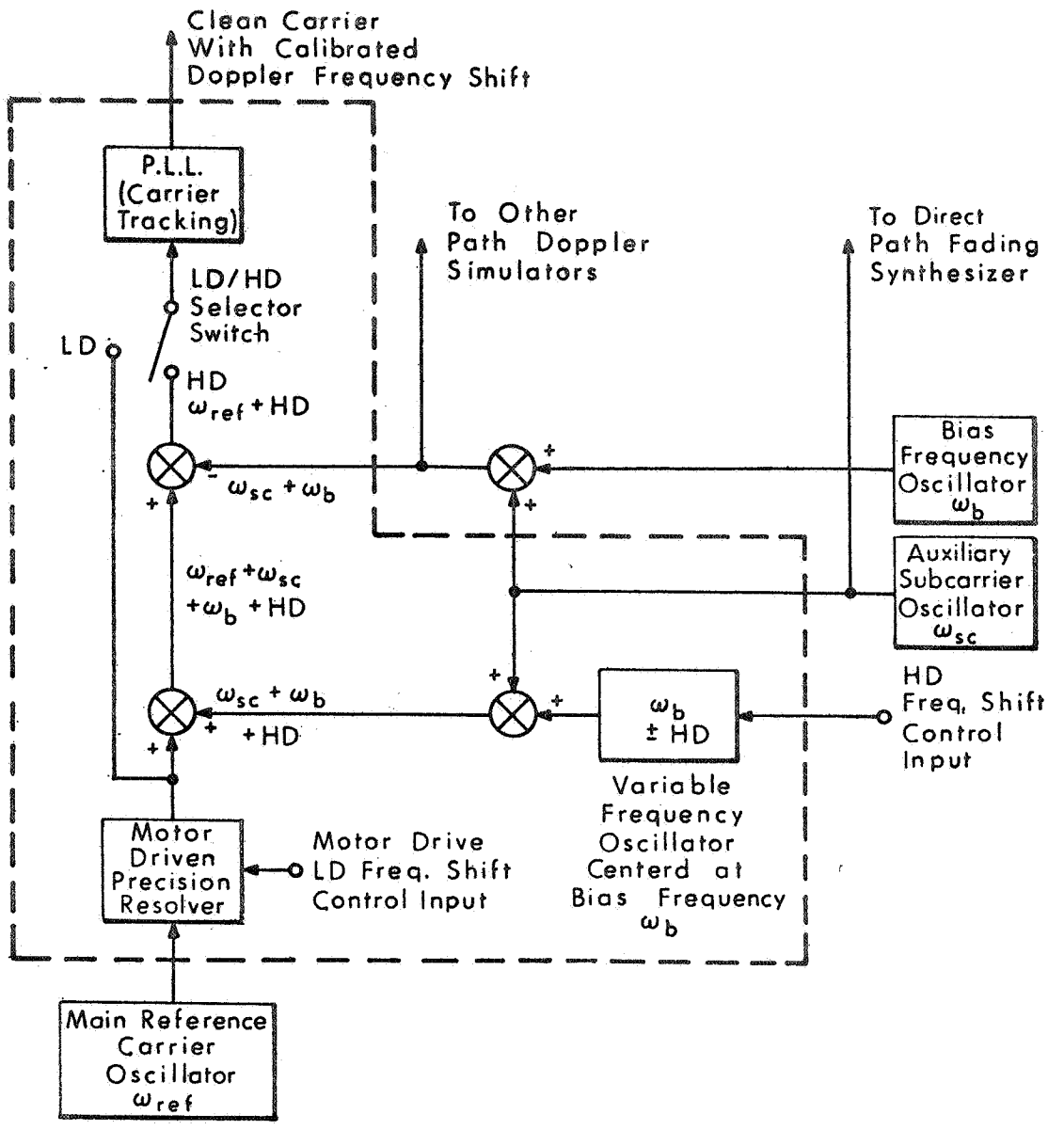

Fig. 12 Methods of Adding Low Doppler (LD) and High Doppler (HD) Calibrated Frequency Shifts to the Operating Carrier Frequency

These conflicting requirements are accomplished by a two-stage process. A bias frequency oscillator at ω_b (on the order of 10 kHz) is mixed with a subcarrier oscillator at ω_{sc} (on the order of 500 kHz) to form the total bias frequency at 510 kHz. A variable-frequency oscillator at 10 kHz is frequency shifted in accordance with the required doppler and mixed with the subcarrier oscillator at ω_{sc} to form the total bias plus doppler frequency. The frequency instability between the reference oscillator at ω_b and the variable-frequency oscillator at ω_b is expected to be sufficiently smaller than the desired doppler offset so that the frequency uncertainty would not amount to more than 10 % for doppler frequencies higher than 10 Hz. The frequency separation problem (i.e., separating 510 kHz from 490 kHz, and 30.51 MHz from 29.49 MHz) is not expected to pose any practical difficulties. If necessary, a carrier-tracking phase-locked loop with a bandwidth of a few hundred Hz can be used to extract a clean carrier from the output of the final mixer.*

4.3.4 Generation of Additive Noises

The box labeled Additive Noise Source will include provisions for generating--under operator selected and calibrated-controlled conditions--three types of noise: gaussian random-fluctuation noise, impulse noise, and interfereing signals. The range of calibrated-controlled conditions for each of these types of noise will be in accordance with realistic specifications, reviewed below under the separate descriptions of the proposed realizations of the additive noise sources.

---

*An alternate doppler simulation technique is presented in Sec. 5. This technique permits "fast" and "slow" doppler to be simulated without the need for resolvers.

Gaussian Random Fluctuation Noise

Gaussian noise, which is white over the channel bandwidth, can be obtained from a silicon junction avalanche-diode.* These diodes can provide very stable wideband sources of gaussian noise having a flat spectrum from several kHz to several hundred MHz. These diodes also exhibit good stability of their output noise as a function of temperature. A temperature coefficient of -0.02 dB per deg F (under conditions of constant junction current) is representative of the diode temperature stability. Avalanche-diode units that have been carefully selected for noise level and spectral flatness are commercially available.

The noise from such a diode can be filtered by an IF bandpass filter that passes only that part of the spectrum corresponding to the channel bandwidth. The noise at the output of the filter can then be amplified to the maximum level required. Calibrated attenuators at the output of the amplifier can be used to obtain any required level of output noise in the specified range from 10 dBm to -50 dBm.

Impulse Noise Generator

The output of the impulse noise generator consists of narrow pulses, each of fixed height and duration, with a mean pulse repetition frequency that is calibrated and adjustable over a wide range (from several pulses per second to approximately one million pulses per second). The impulse generator drives an IF bandpass filter which represents the front-end filtering of the receiver. The amplitude of the impulse noise at the output of this filter is varied in 5 dB steps from +10 dBm to -50 dBm.

*"Why Not the Avalanche Diode as an RF Noise Source," Hays Penfield, Electronic Design, April 12, 1965.

The large range of mean p. r. f.'s required for the randomly occurring pulses necessitates careful design in order to obtain stable mean p. r. f.'s over the entire range. A proposed solution to this problem is shown in the block diagram form in Fig. 13.

A silicon junction avalanche diode is used to provide a stable source of wideband gaussian noise having a power spectral density that is flat from several kHz to several hundred MHz.* This noise is amplified by a feedback amplifier whose gain is adjusted so as to produce an adjustable bandwidth with a constant gain-bandwidth product. The output of this amplifier drives an amplitude discriminator that generates a pulse of fixed height and fixed narrow duration whenever the noise voltage increases through a predetermined level. The dc component of these pulses is a measure of the mean p. r. f.

For a gaussian noise voltage, v(t), the average number of times per second, $n(v_1)$, that v(t) increases through v_1 is

$$n(v_1) = r\, e^{-\frac{1}{2} v_1^2/\sigma^2}$$

where

$$r = \left[\frac{\int_0^\infty f^2 w(f)\, df}{\int_0^\infty w(f)\, df} \right]^{1/2} .$$

is the rms frequency of gaussian noise with spectral density w(f), and

$$\sigma^2 = \int_0^\infty w(f)\, df$$

is the total power.

*This can be the same silicon junction avalanche diode used as the source of gaussian noise in the additive gaussian random fluctuation noise source.

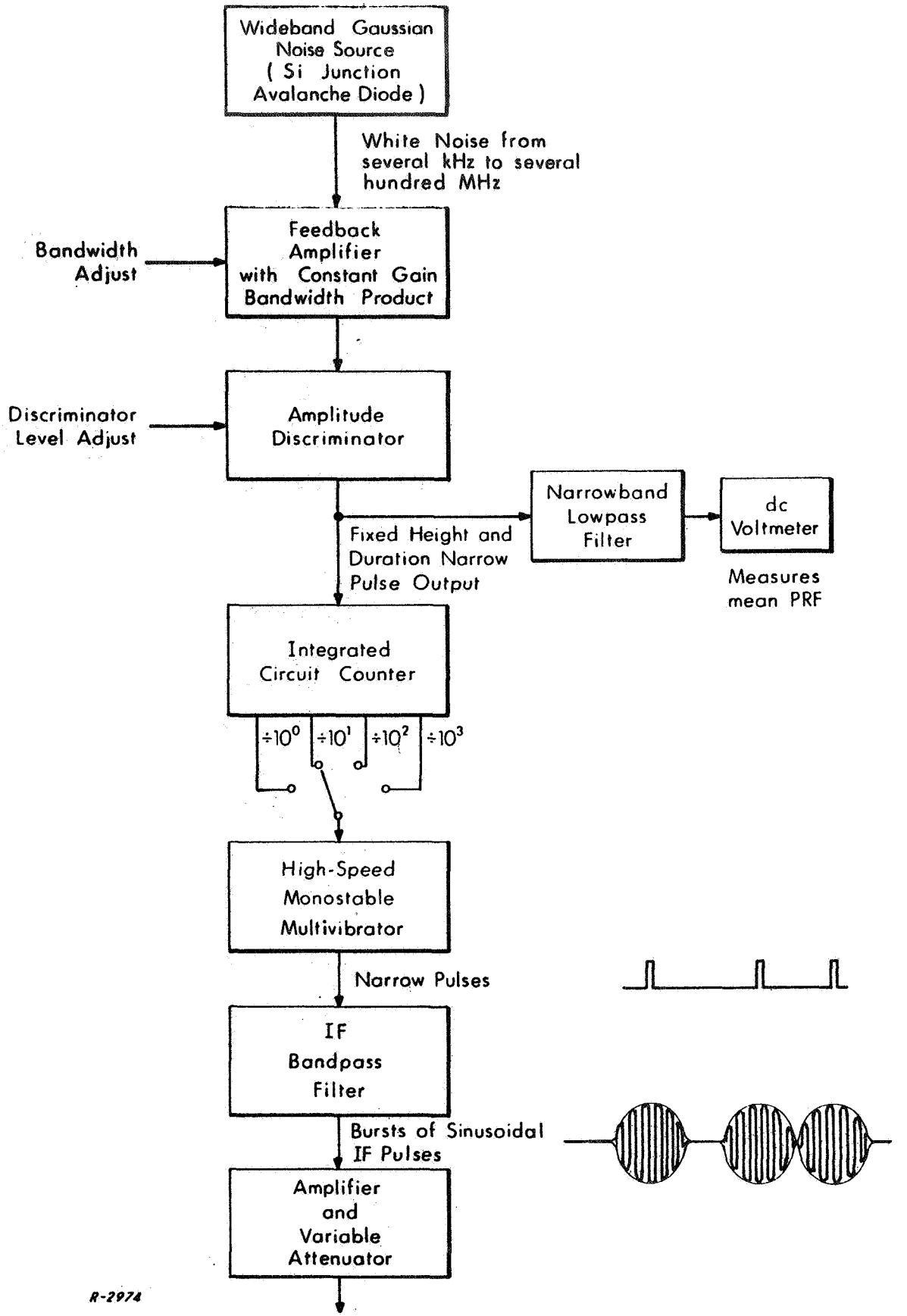

Fig. 13 An Impulse Generator

The mean p. r. f. at the output of the amplitude discriminator can be controlled by varying v_1 and r. The sensitivity of $n(v_1)$ to changes in v_1 is greatest at $v_1 = \sigma$. We propose to use v_1 as a fine control, varying it from $(1/2)\sigma$ to $(3/2)\sigma$. The rms frequency of the noise, r, can be varied in steps by adjusting the bandwidth of the feedback amplifier in steps. The constant gain-bandwidth product of the amplifier insures that σ^2 does not change. The rms bandwidth of the noise, r, can be reduced only to about 10 MHz. Further reductions in the mean p. r. f. can be achieved by using an integrated circuit counter and connecting the input of a monostable multivibrator to whatever output of the counter corresponds to the required range of mean p. r. f.

The heights of the pulses at the output of the IF bandpass filter are then adjusted by a variable attenuator. These pulses may either be mixed or frequency multiplied up to RF.

It is felt that this system can be readily calibrated and stabilized in mean p. r. f. and pulse height over the entire range of desired mean pulse repetition frequencies.

5. A TYPICAL SIMULATOR CONFIGURATION

In this section we present a possible simulator configuration as a vehicle for discussing the critical areas of design: delay, delay spread, doppler, ionospheric fading simulation, and diffuse multipath fading simulation.

The difficulty inherent in delaying an RF (or IF) signal of wide bandwidth (up to 4 MHz) by delays up to 30 msec has led us to consider techniques which effectively produce undelayed and delayed baseband modulation signals. These signals are then modulated onto the carrier by modulators appropriate to the transmitter under consideration. The undelayed (direct-path) signal and the delayed (earth-reflected multipath) signal are then fed into the channel simulator which simulates the other effects on the received signal which arises from the direct-path and the earth-reflected multipath channels.

To illustrate these ideas, assume that the modulation consists of binary coded data which modulates a pseudo-noise waveform to produce a spread spectrum modulating signal which then phase modulates the RF carrier A general system block diagram is shown in Fig. 14. In this general system configuration carriers modulated by undelayed and delayed modulation are produced and fed to a direct-path and an earth-reflected multipath channel simulator, respectively. The outputs of these simulators are the simulated received RF direct-path signal and the simulated received RF specular and diffuse earth-reflected multipath signals. These are added with external noise and interferences in order to simulate the total received RF input to the receiver.

The modulation delay simulator is shown in block diagram form in Fig. 15. The spread spectrum modulator and the carrier modulator are part of the transmitters under test. Two transmitter modulators are necessary

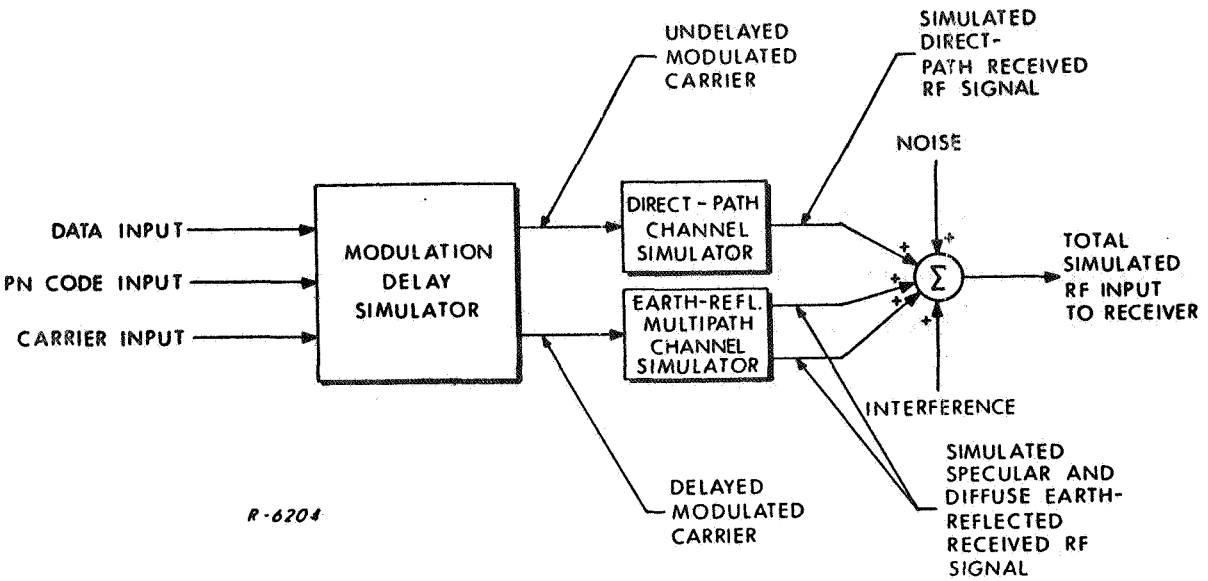

Fig. 14 General System Block Diagram of TDRS-User Spacecraft Channel Simulator

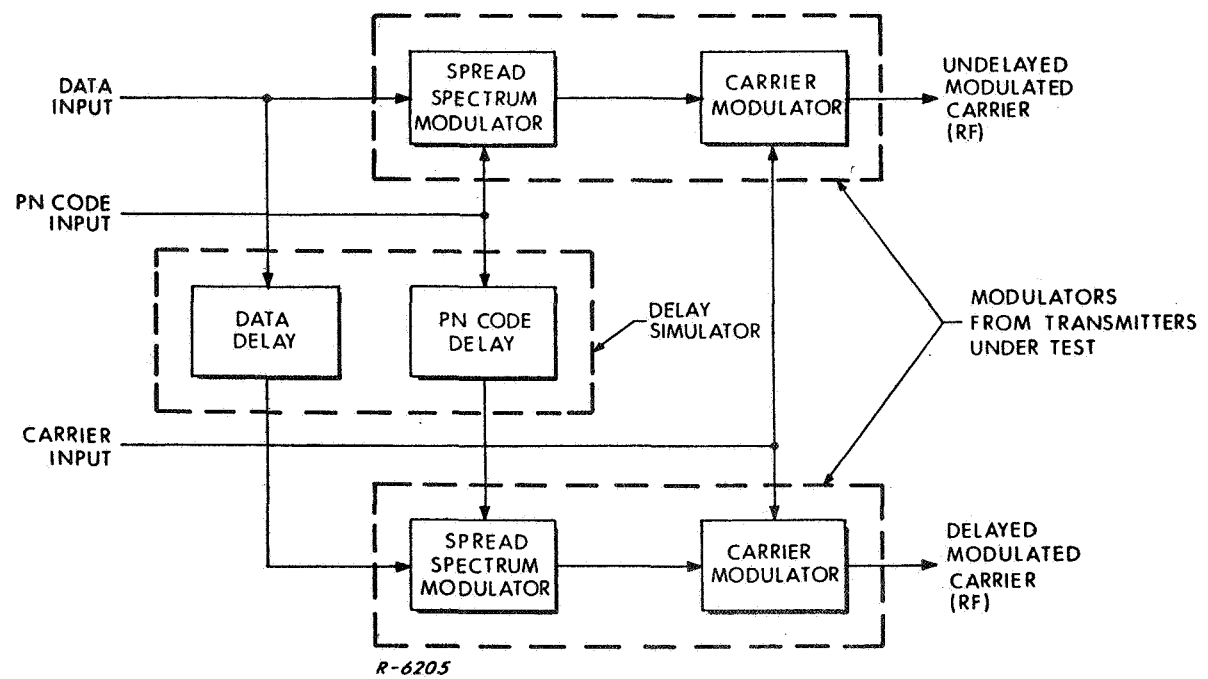

Fig. 15 Modulation Delay Simulator

here as well as a data input, a PN code input, and a carrier input. The heart of the modulation delay simulator is the data delay unit and the PN code delay unit. The operation of these units will be explained shortly.

Turning now to the channel simulators, a block diagram of this portion of the simulator is shown in Fig. 16. The RF input signals are mixed down to a convenient IF frequency by a local oscillator. The direct-path simulator includes an ionospheric fading simulator and a direct-path doppler simulator. The ionospheric fading simulator simulates the effects of slow fading of the direct-path signal as a result of polarization rotation effects and the effects of multiple paths separated by time delays small compared to a period of the highest significant frequency component of the modulation, but perhaps large with respect to a period of the carrier. The doppler simulator puts out a frequency which differs from the input frequency by a known and controlled amount. The carrier doppler is added to the direct path RF signal during the final mixing of the IF up to the original RF. The earth-reflected multipath channel simulator has provision for simulating a constant specular multipath component and a fading diffuse multipath component. The specular multipath component may be attenuated to any level with respect to the direct-path signal, and also contains an additional relative multipath doppler frequency. The diffuse multipath component consists of a sum of 4 or 5 fading components each having a different time delay (delay spread). These simulated RF diffuse multipath components have their spectrums centered around the specular-multipath doppler frequency offset RF carrier frequency as indicated in Fig. 16. The operation of the ionospheric and diffuse multipath fading simulators, the doppler simulators, and the delay spread simulator will be described shortly.

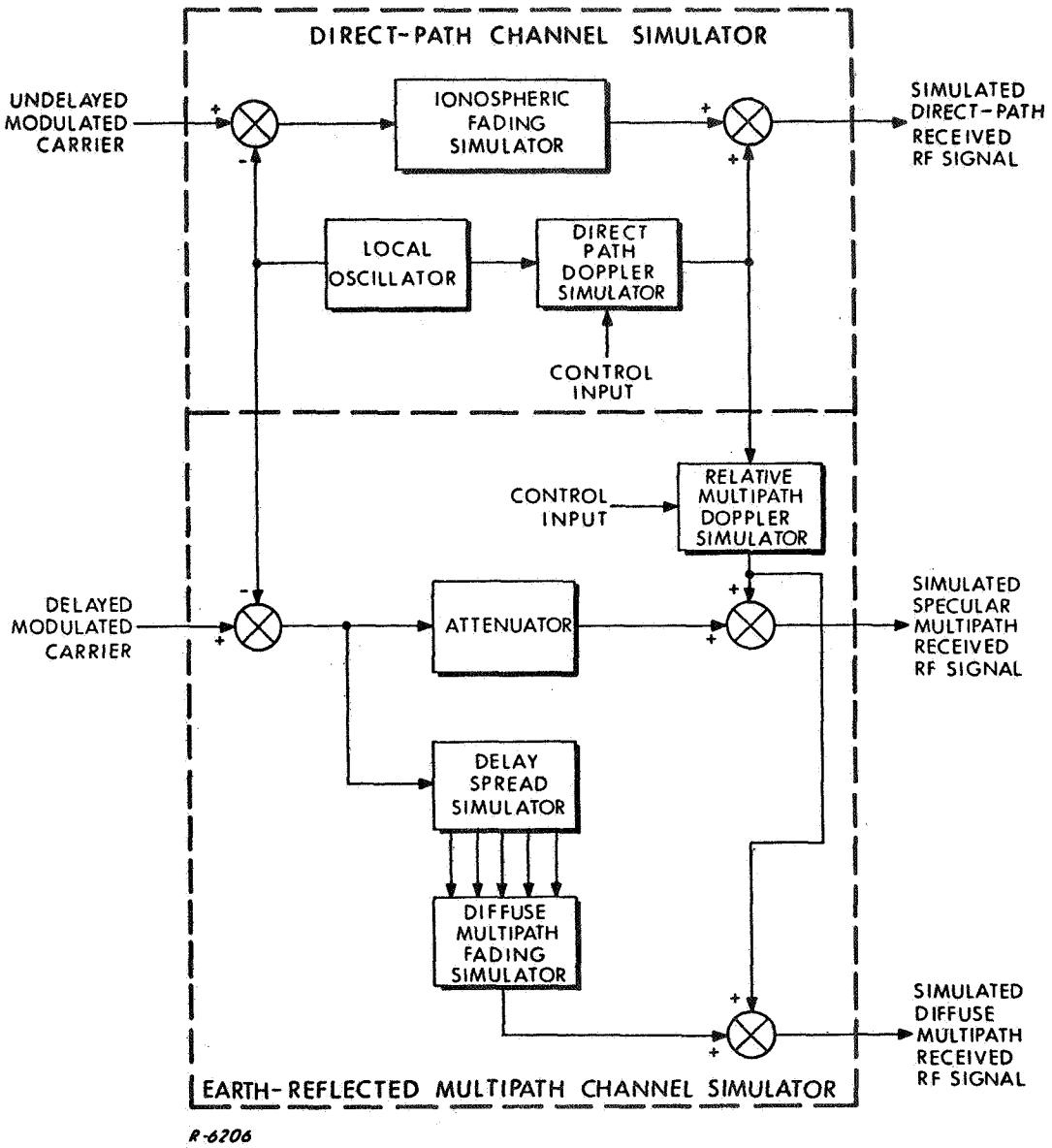

Fig. 16 Channel Simulators

The data delay unit is shown in Fig. 17. It consists of a data clock phase shifter, which permits continuous phase shifting of the clock over a one-bit period, and a shift register which provides a number of outputs each differing in delay by one bit. The number of stages of this shift register equals the number of bit periods contained in the maximum relative delay between the direct-path and the multipath received signal.

The PN code delay unit is shown in Fig. 18. It consists of a PN code generator and a delay unit which delays the starting time of this code generator with respect to the starting time of an input PN code. The code generator has a reset button, an enable input, and a clock input. The reset button places the code generator into an inactive state in which it will remain until the enable signal turns it on. When this occurs, the clock input will drive the code generator starting from its initial state. The enable signal is the "one" output of a flip-flop, and is obtained as follows. The counter and the two flip-flops are reset by reset switches. The counter set switches then set the counter to a predetermined state in accordance with the number of PN code clock periods by which it is desired to delay the code. The flip-flop at the output of the counter is then enabled, and then the flip-flop at the input to the counter is enabled. At the beginning of the PN code sequence a pulse sets the flip-flop at the input to the counter. This enables the counter which then starts counting PN code clock cycles. When the counter reaches the all zero state the output flip-flop is set and this enables the phase shifted clock to drive the code generator which then starts its code sequence.

For the case where a sinusoidal subcarrier is used instead of a PN code, one need only phase-shift the subcarrier in order to obtain the required delay (modulo 2π). The technique used for the PN code delay can be used for any other code so long as the appropriate code generator is used.

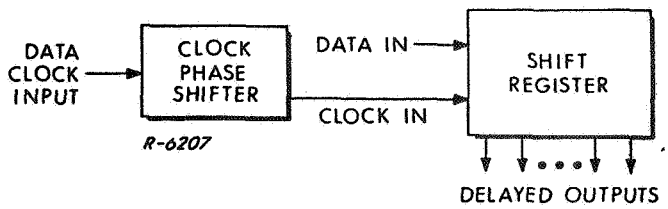

Fig. 17 Data Delay Unit

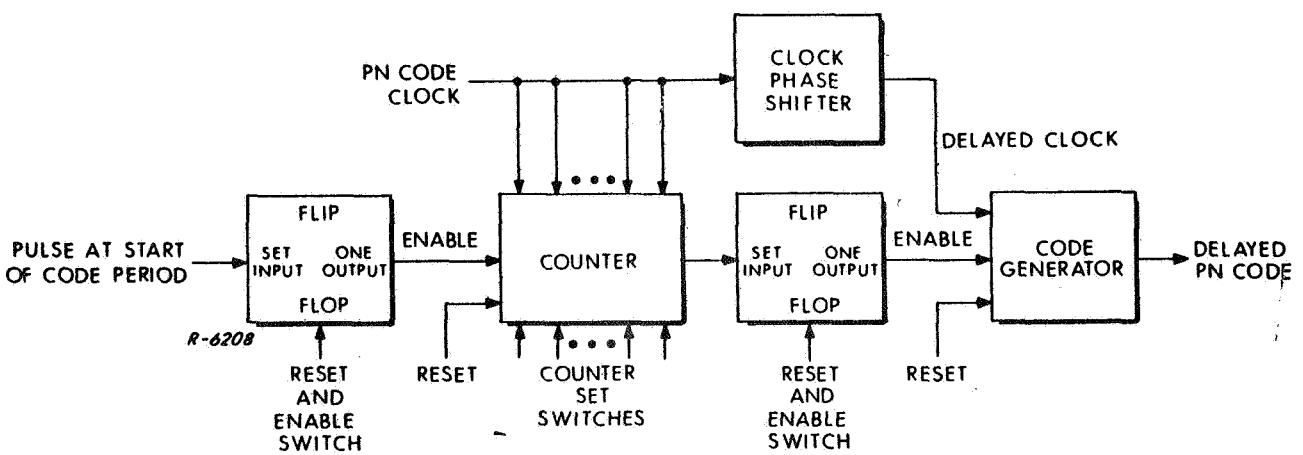

Fig. 18 PN Code Delay Unit

Turning now to the units in the channel simulator, a block diagram of the doppler simulator unit is shown in Fig. 19. This unit has as its output a sinusoidal signal which differs in frequency from an input sinusoidal signal by a controlled amount. The output frequency is obtained from a phase-locked VCO as shown. The difference frequency between input and output is phase-locked to a variable frequency oscillator whose frequency may be accurately set.

The ionospheric fading simulator and the diffuse multipath fading simulator contain one or more fading simulators as shown in Fig. 20. The objective of the fading simulator is to produce signals of the form

$$[x_c(t) + k] \sin[\omega_{IF} t + \theta(t)] + x_q(t) \cos[\omega_{IF} t + \theta(t)]$$

from the input signal $\sin[\omega_{IF} t + \theta(t)]$, where $x_c(t)$ and $x_q(t)$ are statistically independent baseband gaussian-distributed random fluctuations. The constant k is zero for the diffuse multipath case, but may not be zero for the cases of ionospheric fading and specular multipath fading (i.e., a single fading specular multipath component but no diffuse multipath). The 90° phase-shifting and multiplication by gaussian noise is done at a convenient frequency ω_o. Note that the signal inputs to the mixers have AM on them and the control inputs have only PM on them. The baseband gaussian noises are obtained as discussed in Sec. 4.2.

The delay spread simulator consists simply of a tapped delay line having delay taps every microsecond or so. The total delay spread that will be simulated is on the order of at most tens of microseconds.

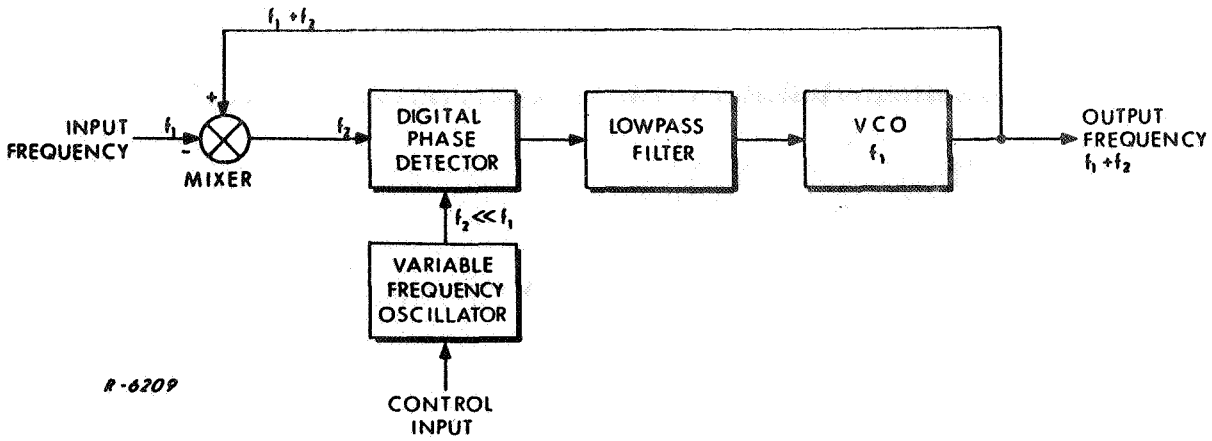

Fig. 19 Doppler Simulator Unit

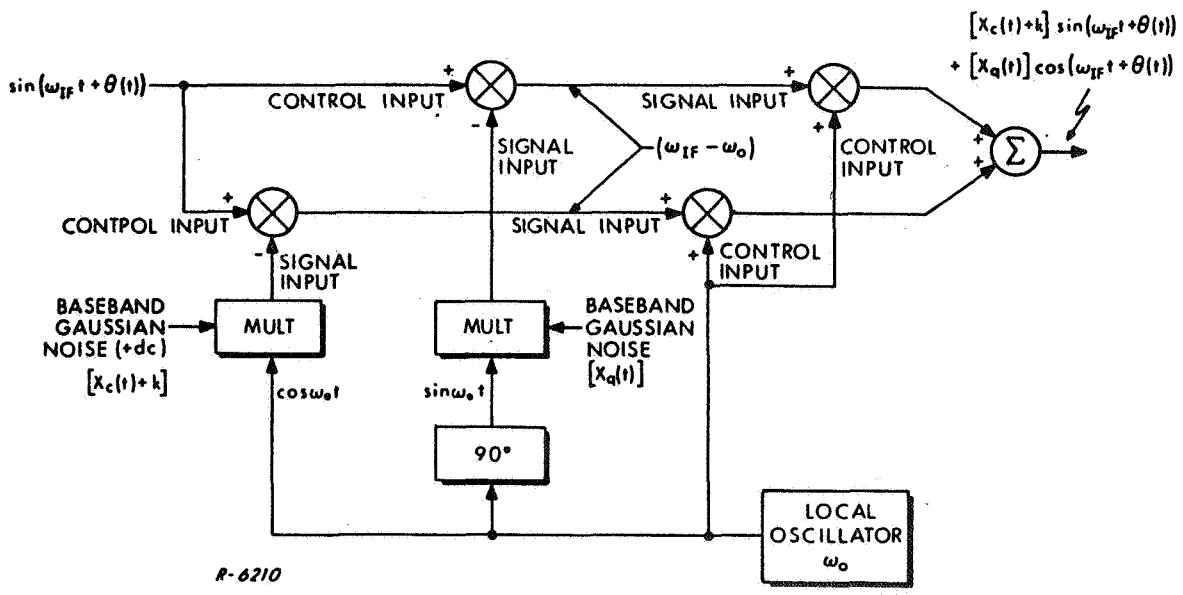

Fig. 20 Fading Simulator

6. SPECIAL PURPOSE SIMULATOR FOR THE WIDEBAND FM DESIRED-USER DIFFUSE MULTIPATH INTERFERENCE

For the situation where the transmitted signal is of the form

$$e_t(t) = \sin\left\{\omega_c t + \beta x(t) + \delta \sin[\omega_{sc} t]\right\}$$

and the multipath time delay spread is much larger than the period of the wideband FM subcarrier, but much smaller than the bit period of the data, a special purpose simulator based on the independently-fading sideband model developed in Technical Memorandum G-161-6 may be used.

The direct-path or LOS signal in this case is

$$e_r(t') = \sin\left\{\omega_c t' + \beta x(t') + \delta \sin[\omega_{sc} t']\right\}$$

where $t' = t - t_d(t)$ is the time-varying LOS delay.

The frequency selective fading multipath interference is represented as

$$e_2\left(t'-t_s(t)\right) = \sum_{n=-N}^{+N} J_n(\delta)\Big[x_{cn}(t)\sin\left\{\left(\omega_c + n\omega_{sc}\right)\left(t'-t_s(t)\right) + \beta x\left(t'-t_s(t)\right)\right\}$$

$$+ x_{qn}(t)\cos\left\{\left(\omega_c + n\omega_{sc}\right)\left(t'-t_s(t)\right) + \beta x\left(t'-t_s(t)\right)\right\}\Big]$$

This signal representation suggests the special purpose simulator shown in Fig. 21. The doppler simulator and the fading simulator are as shown in Figs. 19 and 20, respectively. The sideband filter bank separates the various sidebands so that they can be made to fade independently.

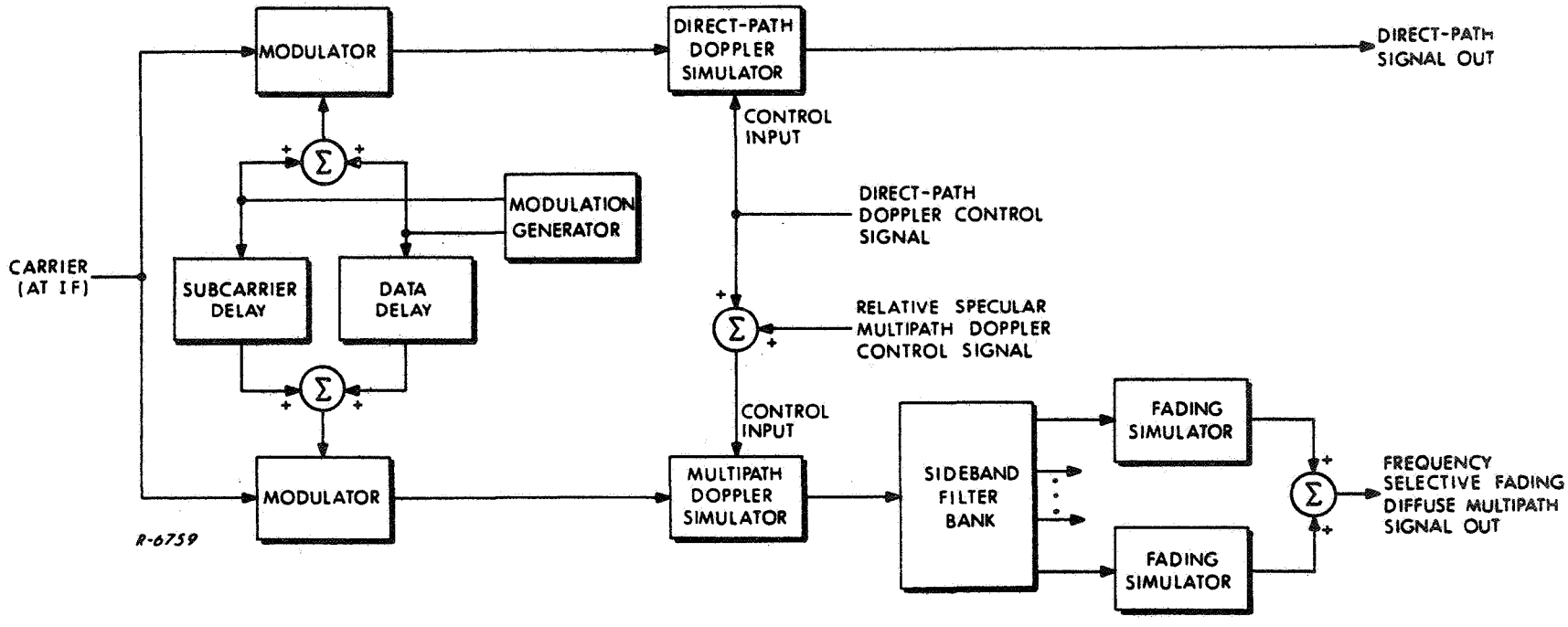

Fig. 21 Block Diagram of Special Purpose Simulator for the Wideband FM Desired-User Diffuse Multipath Interference